



LAWRENCE
LIVERMORE
NATIONAL
LABORATORY

Thermal Infrared Exposure of Cryogenic Indirect Drive ICF Targets

R. A. London, J. D. Moody, J. J. Sanchez, J. D.
Sater, B. J. Haid, D. N. Bittner

July 14, 2005

Fusion Science and Technology

Disclaimer

This document was prepared as an account of work sponsored by an agency of the United States Government. Neither the United States Government nor the University of California nor any of their employees, makes any warranty, express or implied, or assumes any legal liability or responsibility for the accuracy, completeness, or usefulness of any information, apparatus, product, or process disclosed, or represents that its use would not infringe privately owned rights. Reference herein to any specific commercial product, process, or service by trade name, trademark, manufacturer, or otherwise, does not necessarily constitute or imply its endorsement, recommendation, or favoring by the United States Government or the University of California. The views and opinions of authors expressed herein do not necessarily state or reflect those of the United States Government or the University of California, and shall not be used for advertising or product endorsement purposes.

THERMAL INFRARED EXPOSURE OF CRYOGENIC INDIRECT DRIVE ICF TARGETS

R. A. London, J. D. Moody, J. J. Sanchez, J. D. Sater, B. J. Haid
University of California, Lawrence Livermore National Laboratory
7000 East Avenue, Livermore, CA 94550
email: rlondon@llnl.gov

and

D. N. Bittner
Schafer Corporation
303 Lindbergh Ave., Livermore CA 94551

Cryogenic inertial confinement fusion targets at the National Ignition Facility and the Laser Megajoule will be protected from thermal infrared radiation by a cold shroud. As the shroud is removed just before the laser pulse, infrared radiation will heat and possibly degrade the symmetry of the solid hydrogen fuel layer. A lumped component mathematical model has been constructed to calculate how long an indirect drive target can be exposed to thermal radiation before the fuel layer degrades. The allowed exposure time sets the maximum shroud removal time and therefore has important implications for the design of the cryogenic shroud systems. The model predicts that the maximum exposure time is approximately 0.18 s for plastic capsules inside hohlraums with transparent laser entrance holes. By covering the laser entrance holes with a partially reflective coating, the exposure time can be increased to approximately 1 s. The exposure time can be increased to about 2 s by using beryllium capsules. Several other design concepts could increase the exposure time even further. Lengthening of the allowed exposure time to 1 s or longer could allow a significant cost savings for the shroud system.

I. INTRODUCTION

The baseline ignition target designs for the future NIF and LMJ facilities include a solid layer of DT fuel inside a spherical capsule.^{1,2} These cryogenic targets are extremely sensitive to their thermal environment. A cryogenic shroud will surround the targets and protect them from thermal infrared radiation and from condensation. The shroud must be removed just before the laser is fired in order to allow the laser beams to hit the target and to minimize the amount of material near the target that can be turned into shrapnel and thereby damage the final optics. An important issue is how fast the shroud must be

removed. In general, faster shroud removal requires a more complicated and expensive system. The primary process setting the required shroud removal time appears to be heating of the target by thermal infrared (IR) radiation. As the target is heated, the quality (spherical symmetry and smoothness) of the fuel layer will degrade. At some point the quality will be insufficient to enable a symmetric implosion, which is necessary to achieve fusion ignition. In this paper we present a mathematical model to calculate how fast an ICF target will heat up upon IR exposure when the shroud is removed. We use these calculations, along with estimates of the maximum allowable temperature change of the fuel layer to calculate the maximum allowable shroud removal time.

An analysis of the IR warm-up time for cryogenic capsules has previously been done by R. Stephens.³ The present analysis considers different capsule materials and dimensions (plasma polymer CH and Be vs. polystyrene; 100 μm thickness vs. 10 μm). We present a more systematic model for the power balance within the hohlraum, and include the heating of the hohlraum wall and conductive coupling between the capsule and hohlraum wall and between the hohlraum and the cryostat base.

II. LUMPED COMPONENT MODEL

II. A. Components and Equations

We introduce a time-dependent lumped model to describe the IR heating of an indirect drive ICF target. The model includes 3 thermal masses and 2 conducting elements, as illustrated in Figure 1. The thermal masses are: i) the capsule and fuel, ii) the hohlraum and cooling rings, and iii) the cryostat base. The conducting elements are: i) the hohlraum gas (He) and ii) the cooling rods. The

grouping of these components is based on the relative values of the heat capacities and conductivities of the various fundamental components. For example, the conductance between the fuel and the capsule is about 20 times larger than the conductance across the hohlraum gas. We therefore assume that the fuel and capsule have the same temperature and lump their heat capacities together. Since the heat capacity of the fuel and capsule are very high, we ignore the heat capacity of the gas. Similar arguments hold for the other lumped components. With these definitions, and by assuming that the cryostat base temperature is fixed, the heating of the target can be described by two coupled ordinary differential equations for

the temperature changes of the capsule/fuel mass and hohlraum/rings mass:

$$C_c \frac{dT_c}{dt} = P_c - \sigma_g(T_c - T_h) \quad (1)$$

and

$$C_h \frac{dT_h}{dt} = P_h - \sigma_g(T_h - T_c) - \sigma_r(T_h - T_b). \quad (2)$$

In Equations (1) and (2), T = temperature, C = heat capacity, P = absorbed IR power, and σ = conductance. The subscripts for the lumped components are: c = capsule/fuel, g = hohlraum gas, h = hohlraum/rings, and b = cryostat base.

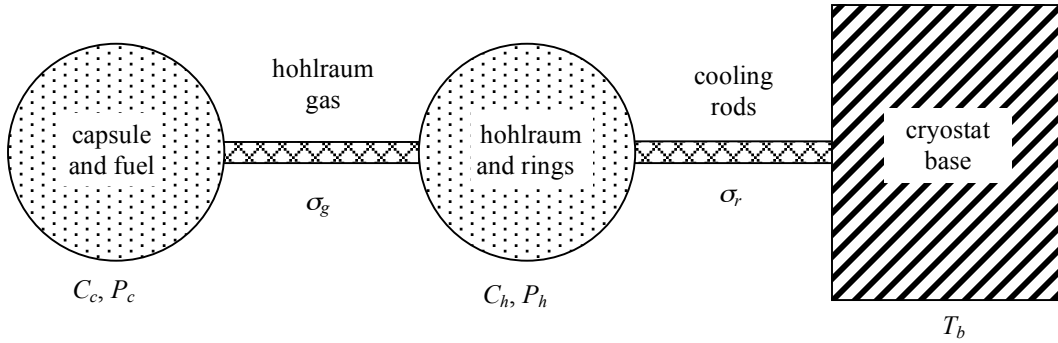


Figure 1. The lumped component model consists of three thermal masses (the capsule and fuel, the hohlraum and cooling rings, and the cryostat base) and two conduction paths (the hohlraum gas and the cooling rods). The thermal masses are assigned heat capacities (C) and power loads (P), while the conduction paths are described by conductances (σ).

II. B. Absorbed IR Power

Upon removal of the cryogenic shroud, we assume that blackbody radiation floods the target chamber and irradiates the target. The flux of radiation striking any exposed surface is given by Stefan's law: $F = \sigma_{sb}T^4$ where σ_{sb} is the Stefan-Boltzmann constant and T is the target chamber wall temperature. The target chamber will be kept at room temperature (294 K), at which $F = 42.4$ mW/cm². The majority of the radiation is in the IR region and the peak of the blackbody spectrum is at 10 μ m. Since the target components are all very cold (≈ 20 K), we can safely ignore re-emission of radiation.

We treat the absorbed IR power in three parts, as shown in Figure 2. The first part is the IR power absorbed by the outer hohlraum walls:

$$P_h = F f_h A_w, \quad (3)$$

where A_w = hohlraum wall area and f_h = hohlraum wall absorption fraction. The area is accurately known from the hohlraum dimensions, while f_h must be estimated

since various non-ideal materials (such as glue, heating wires, etc) are attached to the outside of the hohlraums.

The IR power absorbed by the capsule, P_c , comprises the other two components, defined as the direct and indirect components. The direct component is the radiation absorbed by the capsule immediately upon entering the laser-entrance-holes (LEHs):

$$P_{dir} = F A_{leh} t_{leh} \frac{\Delta\Omega_c}{2\pi} f_c. \quad (4)$$

Here A_{leh} is the LEH area (including both LEHs), t_{leh} is the transmission of the LEH, $\Delta\Omega_c$ is the solid angle subtended by the capsule at a position in the LEH, and f_c is the absorption fraction for radiation hitting the capsule. For the dimensions in Table I, $\Delta\Omega_c/2\pi \approx 2.2\%$. The capsule absorption fraction accounts for rays passing twice through the capsule wall.

Most of the IR that enters the hohlraum hits the wall before hitting the capsule. Part of this radiation scatters around in the hohlraum and gets absorbed by the capsule. We apply a power balance analysis to estimate this indirect power absorbed by the capsule. The power entering

the LEHs but not initially absorbed by the capsule (this is included in P_{dir} above) is equated to the sum of the power absorbed by the wall and capsule and the power exiting the LEHs. The number of reflections of each IR photon can be approximated as the ratio of the area of the hohlraum walls to the sum of the capsule and LEH areas. It is about 8 for the dimensions in Table I. Because this number is large we assume a constant energy density within the hohlraum, E_{hr} . Using the associated energy flux, $F_{hr} = cE_{hr}/4$, we write the power balance equation:

$$FA_{leh} t_{leh}(1 - f_c \Delta\Omega_c / 2\pi) = F_{hr}(A_{leh} t_{leh} + f_c A_c + f_w A_w). \quad (5)$$

The indirect absorbed power is given by $P_{indir} = F_{hr} f_c A_c$. We solve Eq. (5) for F_{hr} and then write the indirect absorbed power:

$$P_{indir} = F f_c A_c \frac{t_{leh} A_{leh} (1 - f_c \Delta\Omega_c / 2\pi)}{f_c A_c + f_w A_w + t_{leh} A_{leh}}. \quad (6)$$

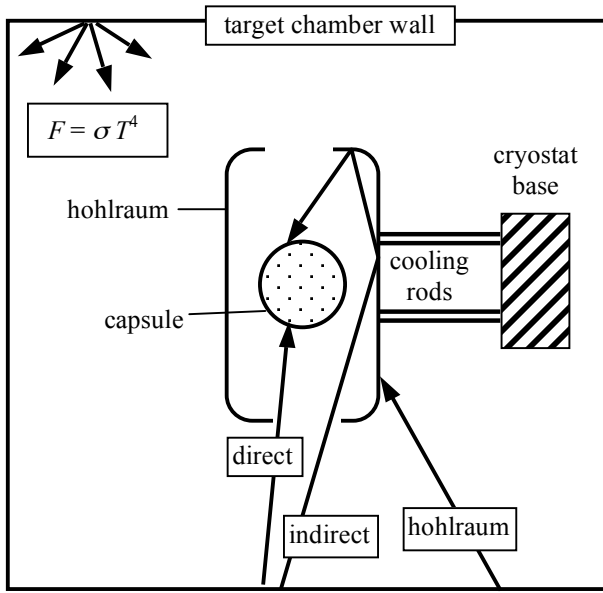


Figure 2. The target chamber emits thermal IR radiation. The target heating is described by three IR components.

II. C. Physical Data

To complete the model we specify the target dimensions and various physical data. The standard values for the target dimensions, used for most of the analysis are listed in Table I.

Values for the IR absorptivities, heat capacities and conductances are derived from basic physical data and from the dimensions of the components and listed in Table II. A range of values is listed for some of the parameters. For the sapphire conductivity, this corresponds to the

variation as the temperature ranges between 15 and 20 K. The range for the absorption fractions (f_c , etc) result from estimates of uncertainties in these parameters.

Table I. Target Dimensions

quantity	value (mm)
capsule radius	1
capsule thickness	0.15
ice thickness	0.10
hohlraum radius	2.75
hohlraum length	9.75
LEH radius	1.375

Table II. Physical Parameter Values

parameter	standard value	range
$C_V(DT)^4$	4 J/g/K	
$C_V(CH)^5$	0.1 J/g/K	
$C_V(Be)^6$	1.3×10^{-3} J/g/K	
$k(He)^7$	2.5×10^{-4} W/cm/K	
$k(sapphire)^8$	T-dependent	35-50 W/cm/K
$f_c(CH)^9$	0.62	0.43-0.81
$f_c(Be)^{10}$	0.1	0.02 - 0.1
f_w^{11}	0.05	0.005-0.05
f_h	0.1	0.1-0.2

The conductivity of the sapphire cooling rods is temperature sensitive. We use measurements made by CEA-Grenoble⁸. To include this effect in the conductance, σ_r , we first fit the conductivity to a power law function: $k = aT^\alpha$. The measured data is fit with $a = 0.4$ W/(cm K $^{\alpha+1}$) and $\alpha = 1.63$ to within 10% for temperatures between 7 and 22 K. We then solve for the temperature distribution along a rod by integrating the steady-state 1-D heat conduction equation with the power law conductivity. The conductance is then found from the ratio of the power to the temperature drop along the rod:

$$\sigma_r = \frac{a}{\alpha + 1} \frac{T_h^{\alpha+1} - T_b^{\alpha+1}}{T_h - T_b} \frac{N\pi r_r^2}{L_r}, \quad (7)$$

where N is the number of cooling rods and r_r and L_r are the radius and length of each rod.

The conductance of the hohlraum gas can be estimated from the conductivity and the capsule and hohlraum dimensions. To get a more accurate value, we have

used 2-D steady state heat conduction simulations, which indicate a value of 0.4 mW/K.

II. D. Absorption by capsule and wall.

For a CH capsule, most of the absorption occurs in the capsule rather than the fuel. Figure 3 shows the wavelength dependent absorption coefficient (κ_λ) determined from transmission spectra of thin CH capsules.⁹ To calculate the wavelength dependent absorption, we assume that IR rays pass directly through the capsule, with a path length equal to twice the shell thickness ($2\Delta r_c$):

$$A_{c,\lambda} = 1 - \exp(-2\Delta r_c \kappa_\lambda). \quad (8)$$

This is also shown in Figure 3. The capsule absorption fraction is then calculated from the blackbody-weighted average of $A_{c,\lambda}$:

$$f_c = \frac{\int A_{c,\lambda} B_\lambda d\lambda}{\int B_\lambda d\lambda}. \quad (9)$$

For a 294-K blackbody spectrum and the absorption coefficient shown in Figure 3, we find $f_c = 62\%$. We estimate an uncertainty in f_c of $\pm 30\%$ (Table II) due to uncertainties in the absorption data and the simplified treatment of the passage of IR radiation through the capsule.

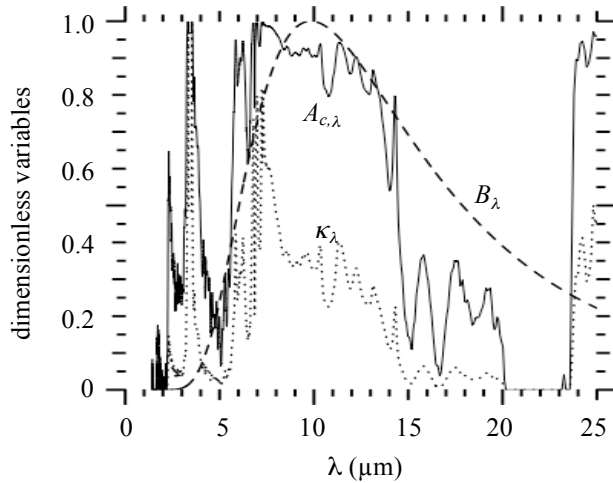


Figure 3. The absorptivity of a CH capsule ($A_{c,\lambda}$) is calculated from the wavelength dependent absorption coefficient (κ_λ) and the Planck function, B_λ . The value of κ_λ is normalized to its peak value of $0.014 \mu\text{m}^{-1}$. The Planck function is also normalized to its peak value.

Absorption by the DT fuel is estimated to be 0.6%—much smaller than absorption by the capsule—and is therefore ignored in our calculations.³

For Be capsules, we treat the absorption fraction as a variable parameter. A pure, polished planar Be surface

has an IR blackbody averaged absorptivity of 2% (ref. 10). An ICF capsule will likely have a larger value, due to heavy element doping and surface roughness. Therefore, we consider values up to 10% to allow for these effects.

The absorption of IR radiation by the inner hohlraum wall is very low. High purity electropolished gold has an absorption fraction of $f_w = 0.5\%$ (ref. 10). However, an actual hohlraum surface will likely not be as pure or smooth as these samples. Therefore, we perform most of our calculations with a higher value of 5% and consider the smaller value as a variation.

Absorption by the outer hohlraum is expected to be dominated by parts attached to the wall such as thermocouples and heating wires. The glue holding these parts is highly absorptive. Therefore the absorptivity, f_h , of the wall will be approximately equal to the fractional area of the wall covered by these parts, estimated to be between 10 and 20%.

II. E. Laser Entrance Hole Transmission

The standard LEH window, a 1000 Å-thick polyimide film to hold gas within the hohlraum, is transparent to IR. However, the film can be coated with a thin metallic layer to reflect IR. We have calculated the Planck-averaged transmission of several coatings using tabulated optical constants¹¹ and the thin film transmission formula.¹² We find that a 50 Å-thick aluminum coating should transmit about 0.5% of the thermal spectrum. The same thickness of gold should transmit 3%. It may be better to use a thicker coating of aluminum, say 200 Å, to overcome oxidation and to further reduce the transmission. The use of an IR reflective LEH coating would make it difficult, but perhaps not impossible, to perform optical characterization of the fuel layer. Therefore, an IR reflective LEH window is more compatible with Be capsules, since they are not amenable to optical characterization in any case. Characterization of the fuel in Be capsules can likely be accomplished with x-ray phase contrast imaging.¹³ If CH capsules are used in conjunction with a reflecting LEH window, one could still use x rays for characterization.

II. F. Comparison to 1-D model

We have compared results of our lumped component model to results of a spherical one-dimensional (1-D) finite element model. The parameters of the 1-D model were chosen to match the masses and dimensions of a Be capsule in a hohlraum. The 1-D model includes heat capacities of the hohlraum gas and of the cooling rods, which are ignored in the lumped model. The 1-D model also includes separation of the capsule and fuel. For a

case in which the laser entrance holes are assumed totally reflecting ($t_{leh}=0$), the temperature-change predictions agree to better than 20% between the two models. The 1-D model predicts that the temperature changes of the capsule and the fuel are within 5%, supporting the lumping together of these components.

III. RESULTS

III. A. Typical Examples

The nature of the target heating is illustrated by two typical examples, one with a CH capsule and one with Be. The parameters for these examples are taken from Table I and the 2nd column of Table II, i.e. $f_w = 0.05$, $f_h = 0.1$, $f_c(\text{CH}) = 0.62$, $f_c(\text{Be}) = 0.1$. For the CH capsules we assume $t_{leh} = 1$, while for Be we take $t_{leh} = 0.1$.

Values of the three absorbed power components are listed in Table III. The indirect absorbed power is much larger than the direct power for both CH and Be. For CH, the IR power absorbed by the capsule is 34 times the beta-decay power, which is approximately 0.04 mW for a 100- μm thick DT layer. In both cases the power absorbed by the outer hohlraum wall is larger than that absorbed by the capsule. However, most of the power absorbed by the hohlraum is conducted through the cooling rods to the cryostat base. As we show below, the dominant effect for CH is heating of the capsule (P_{dir} and P_{indir}), while for Be, the dominant effect is conduction from the hohlraum wall to the capsule.

Table III. Absorbed Power

component	Power (mW)	
	CH	Be
P_{hr}	10	10
P_{dir}	0.066	0.001
P_{indir}	1.30	0.050

Figure 4 shows the temperature histories of the hohlraum wall and the capsule for the two cases. In the first case (Figure 4a), we consider a CH capsule in a hohlraum with transparent LEH windows. The capsule/fuel temperature has been capped at 19.79 K, since our model does not include the melting phase change that occurs in DT at this temperature. For the CH example, the capsule is heated strongly by IR radiation. The capsule temperature initially rises at a rate of 1.4 K/s, a value that can be estimated from the absorbed IR power ($P_{dir} + P_{indir}$) in Table III, and the heat capacity of the capsule/fuel mass (0.98 mJ/K). After a while, conduction to the hohlraum wall moderates the temperature rise. However, this is too late, since we expect degradation of the fuel ice layer, certainly at a temperature rise of less than 1 K.

The second limiting case is illustrated in Figure 4b. This is a Be capsule with a 10% transmitting LEH. Here the IR heating of the capsule is weak. The hohlraum wall heats up first and then conducts energy to the capsule. The rate of temperature rise and the maximum temperature are much lower than for the first case.

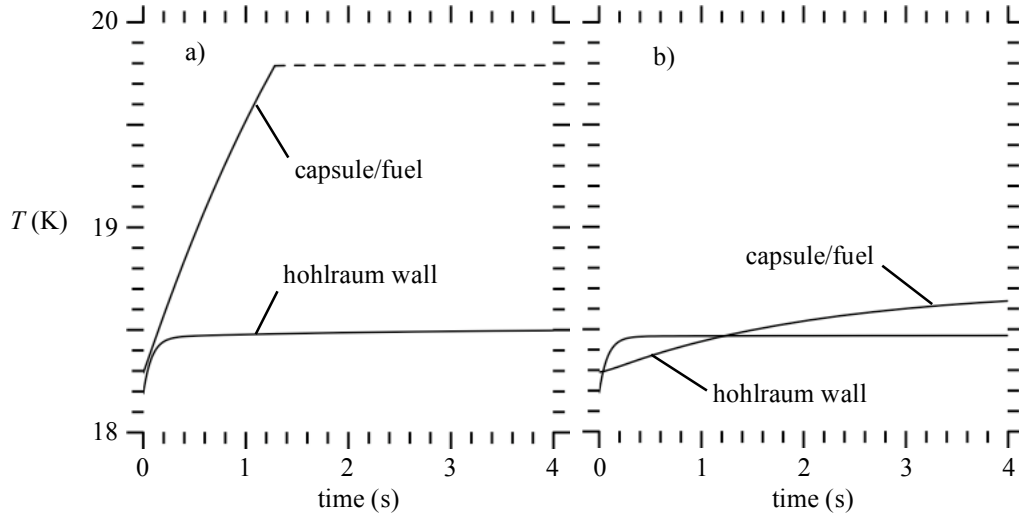


Figure 4. The temperatures of the capsule/fuel component and the hohlraum/rings component are plotted versus time for two cases. Panel 4a is for a CH capsule with LEH transmission, $t_{LEH} = 1.0$. Panel 4b is for a Be capsule with $t_{LEH} = 0.1$, capsule absorption, $f_c = 0.1$ and outer hohlraum wall absorption, $f_{hr} = 0.1$.

III. B. Maximum Allowed IR Exposure.

To set the maximum exposure time, we first specify the maximum temperature rise that can be tolerated before the smoothness of the fuel layer degrades. To estimate the maximum temperature rise, we utilize previous experiments in which HD layers were formed and then slowly cooled 1.5 K below the triple point under IR illumination in a layering sphere.¹⁴ After the cool-down, while still under IR illumination, the layer was warmed by changing the layering sphere temperature in 0.25 K steps. Layer degradation was observed around the fill tube with the first temperature step. We take this value of 0.25 K for the maximum temperature rise, realizing that it is uncertain and should be pinned down in a more specific experiment.

We estimate maximum exposure time by finding when the calculated temperature rise exceeds the maximum allowed rise, as shown in Figure 5 for several cases. The temperature axis is now cut off at a value of $\Delta T = 0.25$ K. Results for these and other cases are summarized in Table IV. For a CH capsule with no LEH reflection, the maximum IR exposure time is 0.18 s. However, by using a 90% reflecting coating on the LEH window, we can extend the time to 0.95 s. With Be capsules, the allowed exposure times are longer, ranging from 1 to 2 s for cases shown in Figure 5.

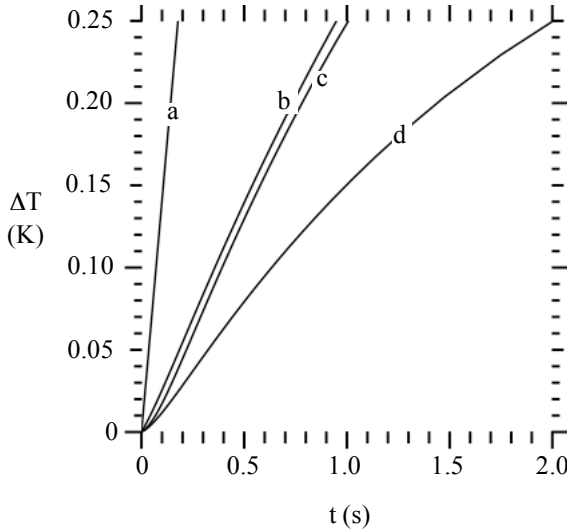


Figure 5. The temperature rise of the capsule/fuel component is shown for four cases listed in Table IV. The maximum tolerable temperature rise before the fuel layer degrades is estimated to be 0.25 K.

Other parameters have been varied, as listed in Table IV. For a CH capsule, decreasing the inner wall absorptiv-

ity (f_w) from 5% to 0.5% reduces the exposure time by 29% due to an increased fraction of IR absorbed by the capsule. Increasing the capsule absorption by 30% causes a decrease in the exposure time by 16%, while a similar decrease in f_c causes a 31% increase in $t_{0.25}$. Completely blocking the LEH ($t_{leh}=0$) increases the exposure time to 5.7 s. For Be, reducing the capsule absorption to 2% increases the exposure time to 3.5 s, while blocking the LEH completely allows an exposure time of 4.7 s.

Table IV. Maximum IR Exposure Times

case (Fig. 5)	material	variation ^a	$t_{0.25}$
a	CH	—	0.178
b	CH	$t_{leh} = 0.1$	0.950
—	CH	$f_c = 0.43$	0.233
—	CH	$f_c = 0.81$	0.148
—	CH	$f_w = 0.005$	0.126
—	CH	$t_{leh} = 0$	5.690
d	Be	—	2.004
c	Be	$f_h = 0.2$	1.007
	Be	$t_{leh} = 0$	4.722
	Be	$f_c = 0.02$	3.529

^aparameter variations with respect to the examples discussed in §III A.

III. C. Increasing the Allowed Exposure Time

Several methods might be used to reduce the heating rate of the target, thereby increasing the allowed IR exposure time. One method is to reduce the IR absorption of the hohlraum. The calculations presented in §III B assumed an absorption fraction of 10% or 20%. It is likely that the absorption can be reduced further by coating the hohlraum and attached components (cooling rings, heaters, thermal sensors) with a thin layer of a highly reflective material, such as Al or Au, as discussed in §II E for the LEH. It also appears possible to reduce the LEH transmission to essentially nil with 50-200Å metallic coatings. As shown in Table IV this would allow approximately 5 s IR exposure time.

Another method to decrease the temperature rise of the capsule is to reduce the electrical power delivered to the hohlraum at the same time the IR exposure begins. In the standard target design, electrical heaters are to be used to control the hohlraum temperature and to control the low mode (1st and 2nd Legendre modes) temperature asymmetry of the fuel layer. The total control power is estimated to be about 50 mW. Since this is somewhat

larger than we expect from IR heating (10-20 mW), the electrical power could be quickly turned down as the shroud is removed to compensate for the IR heating. This might be done using a real time temperature controller, or in a pre-programmed mode, where the correct power decrease is determined by experiments on surrogate targets. Reducing the electrical power helps extend the exposure time for either CH or Be capsules, particularly in the case that the laser entrance holes are covered so that the IR heating of the capsule is minimal.

IV. DISCUSSION AND CONCLUSIONS

We have presented a theoretical model that describes heating of indirect drive ICF targets upon exposure to thermal IR radiation. This model is relevant to exposure when the cryogenic shroud is removed just prior to the firing of the laser beams. We find that the maximum IR exposure time is quite short (0.18 s) for standard CH capsules. We present several methods that can lengthen the allowed exposure time to of order 1-5 s, including using Be capsules and using a partially reflective coating on the laser entrance hole windows for either CH or Be capsules. Other methods such as coating the hohlraum with a reflective coating and reducing the electrical heating power to the hohlraum at the time of shroud removal could further lengthen the allowed exposure time. Given the results presented in §III B and the additional techniques to reduce the IR heating discussed in §III C, it should be possible to achieve 1 s or longer allowed IR exposure times for indirect drive ignition targets. Lengthening the allowed IR exposure time from 0.18 to 1 s could enable the use of a less expensive shroud system for indirect drive targets on the National Ignition Facility.

The results of this study are purely theoretical at this point. We suggest that experiments be done to test the predictions. Measurements of the IR properties of the various materials (CH and Be capsules, hohlraum wall and hohlraum assembly, thin metallic LEH coatings) would be useful. It would be particularly relevant to make such measurements at cryogenic temperatures (≈ 20 K). A second type of experiment would be to measure the maximum allowable temperature rise of a capsule before the fuel layer quality degrades. This could be done by creating a high quality fuel layer in a capsule with either beta- or IR-layering, and then turning on a supplemental IR radiation source (such as a 2nd IR laser or a thermal IR source), to simulate the effect of IR heating upon shroud removal. The third type of experiment is an integrated shroud removal experiment with a cryogenic, layered target, but done in a test facility other than the main laser target chamber.

ACKNOWLEDGMENTS

We are pleased to thank B. Kozioziemski and L. Hagler for helpful discussions. This work was performed under the auspices of the U.S. Department of Energy by the University of California, Lawrence Livermore National Laboratory under contract W-7405-Eng-48.

REFERENCES

1. S. W. HAAN, *et al.*, "Update on Specifications for NIF Ignition Targets and their Rollup into an Error Budget," *Fusion Sci. Technol.* (this volume).
2. PH. BACLET, *et al.*, "The Research Program for the LMJ Cryogenic Target: Main Results and Prospects," *Fusion Sci. Technol.* (this volume)
3. R. B. STEPHENS, "Warm-up Time for Cryo Targets," General Atomics memo (1994).
4. P. C. SOUERS, *Hydrogen Properties for Fusion Energy*, p. 96 (UC Press, Berkeley, 1986).
5. G. HARTWIG, *Polymer Properties at Room and Cryogenic Temperatures*, p. 63 (Plenum Press, New York, 1994).
6. G. AHLERS, "Heat Capacity of Beryllium Below 30 °K," *Phys. Rev.*, **145**, 419 (1966).
7. J. G. WEISAND II, ed., *Handbook of Cryogenic Engineering*, p. 25 (Taylor and Francis, Phila., 1998).
8. M. ROUSTAN, H. ROUILLON, and M. DESMARIS, "Saphir Mesure de Conductivité Thermique," Note SBT/CT/99-41, CEA-Grenoble (1999).
9. R. COOK, M. ANTHAMATTEN, S. LETTS, A. NIKROO, and D. CZECHOWICZ, "IR Absorptive Properties of Plastic Materials Used in ICF Capsules," *Fusion Sci. Technol.*, **45**, 148 (2004).
10. M. BASS, editor, *Handbook of Optics*, Volume II, p. 35.33 (McGraw-Hill, New York, 1995).
11. E. D. PALIK, ed., *Handbook of Optical Constants of Solids* (Academic Press, San Diego, 1998).
12. M. BORN and E. WOLF, *Principles of Optics*, Sixth Edition, p. 161 (Pergamon Press, New York, 1980).
13. B. J. KOZIOZIEMSKI, *et al.*, "X-ray Imaging of Cryogenic Deuterium-Tritium Layers in a Beryllium Capsule," *J. Appl. Phys.*, in press (2005).
14. D.N. BITTNER, G.W. COLLINS, and J.D. SATER, "Generating Low-Temperature Layers with Infrared Heating," *Fusion Sci. Technol.*, **44**, 749 (2003).